

Proceedings of Tailings and Mine Waste 2023 November 5-8, 2023 | Vancouver, Canada

Use of CPT with Dual Pore-Water Pressure Filter Elements in Characterization of Mine Tailings

Iván A. Contreras PhD., P.E., Barr Engineering Co., USAJason W. Harvey, P.E., Barr Engineering Co., USADafar N. Obeidat, Barr Engineering Co., USA

Abstract

The paper presents the results of a series of cone penetration test (CPT) with dual filter element locations $(u_1 \text{ and } u_2)$ performed at three tailings management facilities. Typical results of CPT soundings are presented, discussed, and assessed regarding the features observed and the relationship to tailings characterization, state, sensitivity, aging, and stress history.

Data were assessed and analyzed for general trends in the following three aspects: 1) Behavior of the tailings material in the proposed Robertson's chart and their measured pore-water pressure difference (u_2 - u_0) versus (u_1 - u_0); 2) Pore-water pressure dissipation (PPD) test results; and 3) Measured pore-water pressure difference (u_1 - u_0) as it compares to the susceptibility in terms of compressibility using Olson (2009) relationship.

Introduction

The cone penetration test (CPT) is an in-situ testing tool extensively used in geotechnical investigations of mine tailings. The most basic piezocone typically measures the tip resistance (q_c), the sleeve side resistance (f_s), and pore-water pressure during penetration (u). Additional sensors have been incorporated into more sophisticated piezocones to measure inclination, lateral stress, seismic waves, electrical resistivity, heat flow, radioisotopes, and acoustic noise (Lunne et al. 1996). The measured pore-water pressure during penetration (u) includes the in-situ pore water pressure (u_0) and the components induced by octahedral normal (Δu_{oct}) and shear-induced pore pressure (Δu_s) according to Mayne et al. (1990). As a result, in addition to in-situ pore pressure, values of u in natural soils are an indication of alteration and/or destructuring of the soil structure which likely include sensitivity, stress state, stress history, cementation, and aging among other factors. However, the location of the porous element on the cone significantly affects the measured value of pore-water pressure (u). In the 1990s the filter element location u_2 (i.e. behind the cone tip) was adopted as the standard.

Mine tailings are the waste material from mineral processing (i.e., crushing, grinding, and separation) of ore and are conventionally slurry discharged in the tailings storage facility (TSF). Mine tailings consist of material with particle sizes ranging from coarse (i.e., sand-size) to fine (i.e., silt-size to clay-size). Slurry tailings tend to exhibit contractive behavior and thus are susceptible to liquefaction due to their method of deposition, geologic age, and stress history of these deposits (Terzaghi et al., 1996). These depositional conditions and material characteristics generate high variability of tailings deposits and properties, which pose technical challenges for determining state, sensitivity, and undrained shear strength (Contreras and Harvey, 2021).

It was thought that CPT capable of measuring pore-water pressures at two locations (u_1 and u_2) would provide insights about tailings characterization, state, sensitivity, aging, and stress history. A comprehensive field investigation program was conducted across three (3) different tailings storage facilities (TSFs) using CPT with dual pore-water pressures filter element locations (u_1 and u_2). This paper presents the results and interpretation of the investigation and discusses the different aspects of the findings in relation to tailings characterization, state, aging, and stress history as well as other behavior factors.

Pore-water Pressure Generation During CPT Penetration

CPT penetration generates changes in the pore-water pressure conditions in the area surrounding the cone. CPT penetration in saturated soils with low permeability (i.e., hydraulic conductivity) such as clays, occurs under undrained conditions. The variation in pore-water pressures is the result of a combination of changes of the octahedral normal stress, $\Delta\sigma_{oct}$, resulting from the displacement of soil and water as the cone penetrates the ground, and the octahedral shear stress, $\Delta\tau_{oct}$, caused by the shear deformation adjacent to the cone penetrometer (Burns and Mayne, 1998).

According to Baligh (1986), at the cone tip the largest impact on pore-water pressure magnitude is due to compression or change in mean normal stress with small contribution in relative changes in shear stresses (i.e., <20%). On the other hand, along the cone shaft the shear stresses are a more significant portion of the induced excess pore-water pressures as the octahedral normal stresses at the tip undergo stress relief at the shaft. Therefore, the area in shaft behind the cone tip is more affected by shear stresses than the area of the tip (Wroth 1984; Campanella et al. 1986).

In mine tailings which include material with particle sizes ranging from coarse (i.e., sand-size) to fine (i.e., silt-size to clay-size) the CPT penetration does not always occur under undrained conditions. In fact, depending on the material, the penetration may be drained, undrained, or partially drained. In some instances, fast CPT penetration is used to assess drainage and its impact on measured parameters (Contreras

and Grosser, 2009). In any event, still remains as a combination in changes in octrahedral normal stress.

The total magnitude of pore-water pressure measured during CPT includes the in-situ pore water pressure (u_{θ}) and the components induced by octahedral normal (Δu_{oct}) and shear induced pore pressure (Δu_s) . These contributions can be represented by Equation (1) as follows:

$$u = u_0 + \Delta u_{oct} + \Delta u_{s} \tag{1}$$

When the groundwater conditions are known by means of piezometers, u_{θ} is known. Theoretically, the individual components of Equation (1) can be separated. However, in the field a single total measurement, u, is obtained and separate measurement of the components (Δu_{oct} and Δu_{s}) cannot be performed.

Field Investigation Program

A comprehensive field investigation program was conducted across three (3) different tailings storage facilities (TSFs) using CPT with dual pore-water pressures filter element locations (u_1 and u_2). The in-situ testing involved a series of CPT soundings and soil borings adjacent to each other; with nearly continuous disturbed samples collected for index testing and correlation development. In addition to CPT, shear wave and compression wave velocity measurements and field vane shear test (FVT) were conducted at discrete depths in borings. At each TSF two testing and sampling locations were developed. Each testing location included the following: one continuous CPT with dual pore-water pressures filter element locations (u_1 and u_2), one CPT for measurement of shear and compression wave velocity Vs and pore-water pressure dissipation (PPD) at one meter intervals, one soil boring with nearly continuous sampling for laboratory index testing, and four (4) adjacent soundings with FVT measurements at discrete intervals. A total of 6 continuous CPT soundings with dual pore-water pressures filter element locations were performed as part of the investigation and are used in the interpretation and assessment of the data. The in-situ pore-water pressure regime (u_0) was very well established at each testing location based on the measurements using nested vibrate wire piezometers.

Different pore-water pressure parameters have been proposed by researchers for the interpretation of piezocone soundings with dual filter elements (i.e., Jamiolkowski et al., 1985; Campanella and Robertson, 1988; Mayne et al. 1990; Burns and Mayne 1998). Some of these parameters include $\Delta u = (u - u_0)$, $q_c - \sigma_{vo}$, $q_t - \sigma_{vo}$, u/q_c , u/u_0 , $u/u_$

Figure 1 shows a typical CPT with dual pore-water pressure filter results in mine tailings. Figure 1a shows the corrected cone tip resistance q_t versus depth at one of the TSF. In Figure 1a the trace of the corrected tip resistance, q_t , is represented in light gray but there are three distinct zones with traces using different colors, red, green, and blue. The red trace represents the slimes material located in the following depth intervals 8.7 to 11.3m and 26.8 to 29.3 m. The green trace represents the fine tailings material located in the following depth intervals 20.70 to 22.4m and 24.1 to 25.2 m. The blue trace represents the interbedded mix of slimes and fine tailings material located in the following depth interval 12.2 to 14.3m.

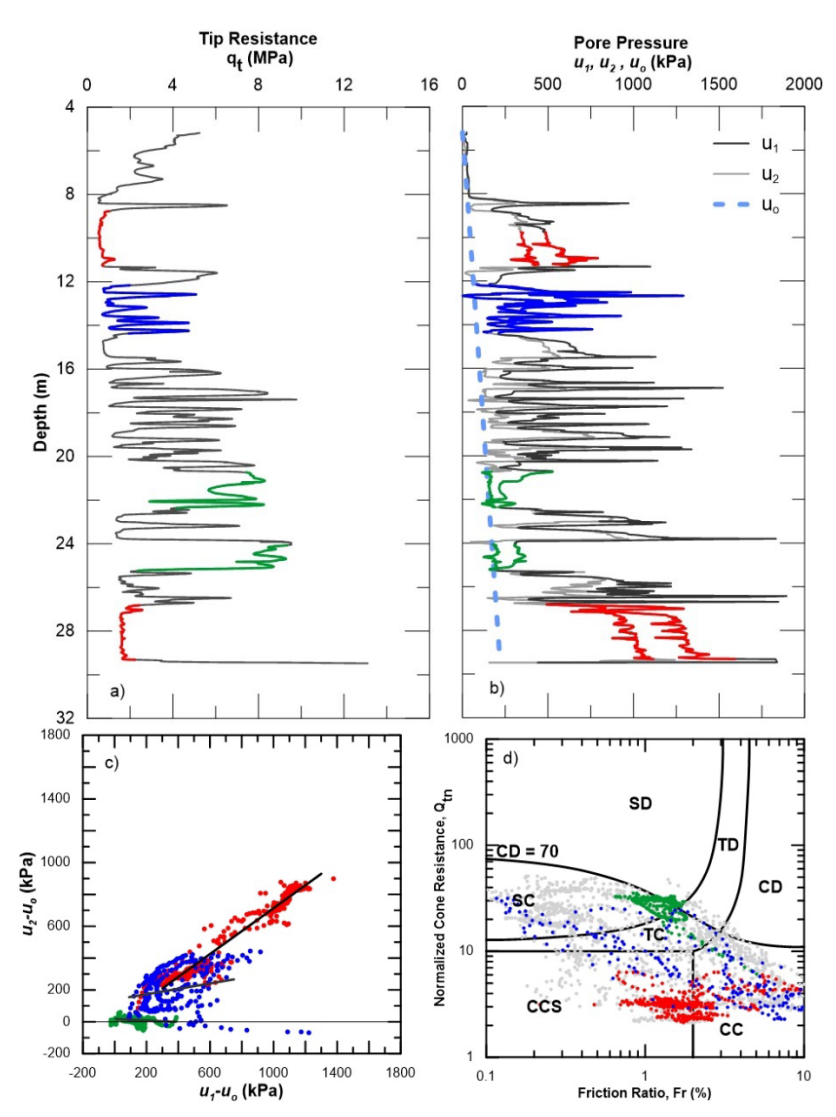


Figure 1: A Typical CPT With Dual Pore-Water Pressure Filter Results in Mine Tailings

Figure 1b shows the measured pore-water pressure at filter locations (u_1 and u_2) and the in-situ porewater pressure profile (u_0) obtained from vibrating wire piezometers at the section. In Figure 1b, the traces of the measured pore-water pressure at both filter locations are shown in black for u_2 and light gray for u_1 In most of the profile. The in-situ pore-water pressure profile (u_0) is shown in a light blue dashed line. However, there are three distinct zones within traces using red, green, and blue colors, same as in Figure 1a. The pore-water pressure traces of the slimes (i.e., red) show u_1 greater than u_2 both increasing with depth, both being greater than u_0 , and consistently u_1 being greater than u_2 within the interval suggesting undrained conditions during piezocone insertion. The pore-water pressure traces of the fine tailings (i.e., green) show u_1 greater than u_2 , u_2 being almost on top of the u_0 trace, and consistently u_1 being greater than u_2 within the interval. The gap or difference between $(u_1$ and $u_2)$ is smaller in the fine tailings than in the slimes. Finally, the pore-water pressure traces of the interbedded mix of slimes and fine tailings (i.e. blue) show behavior with a combination of the observed for the slimes and fine tailings.

Figure 1c shows the measured pore-water pressure difference (u_2 - u_0) versus (u_1 - u_0) from the profile in Figure 1b. To facilitate the interpretation the difference is presented only at the three distinct zones previously discussed. The pore-water pressure in the slimes (i.e., red) shows a fairly consistent trend line of increasing (u_2 - u_0) with the increase of the difference (u_1 - u_0). The average slope of this line is approximately 0.72. On the other hand, The pore-water pressure in the fine tailings (i.e., green) shows a fairly flat line with small variations of (u_2 - u_0) with the increase of the difference (u_1 - u_0). Finally, the pore-water pressure in the interbedded mix of slimes and fine tailings (i.e. blue) show an erratic behavior with jumping values of (u_2 - u_0) with different (u_1 - u_0) which reflect a combination of the observed response of the slimes and fine tailings.

Figure 1d shows the results from the CPT behavior chart proposed by Robertson (2016) which utilizes the normalized corrected tip resistance Q_{tn} and the friction ratio F_r . From characterization standpoint, Robertson's chart classifies the material in sand-like behavior and clay-like behavior separated with the transitional material between the two. Each material group is then separated between dilative and contractive based on the CD line of 70. The three distinct traces previously discussed, are indicated in Figure 1d with the red, blue, and green colors for consistency. The rest of the points of the CPT sounding are shown in light gray. From characterization standpoint, the slimes (i.e., red) are within CC and CCS zones which correspond to Clay Contactive (CC) and Clay Contractive Sensitive (CCS). The fine tailings (i.e., green) are mostly within the SC and some in the TC which correspond to Sand Contractive (SC) and Transition Contractive (TC). The mixture of fine tailings and slimes (i.e., blue) is between the fine tailings and slimes and within the Sand Contractive (SC), Transition Contractive (TC), and Clay Contractive (CC) with some in Clay Contractive Sensitive (CCS). All the data except for few points are below the CD 70 line indicating that all the material is contractive.

Results of Measurements and Trends

Data from 6 CPT soundings at four different TSF were compiled and processed to assess general trends and behavior of the mine tailings deposits. The tailings from the four TSF were deposited using slurry deposition. The main deposition method at the four TSF was mostly subaqueous in general. However, at two of the TSF facilities there was some subaerial aerial deposition and also exposure of the tailings to air drying which contributed to development of desiccation crust at different periods before resuming deposition.

Data were assessed and analyzed in the following three aspects: 1) Behavior of the tailings material in the proposed Robertson's chart and their measured pore-water pressure difference (u_2-u_0) versus (u_1-u_0) ; 2) PPD test result; and 3) Measured pore-water pressure difference (u_1-u_0) as it compares to the susceptibility in terms of compressibility using Olson (2009) relationship.

Robertson's Chart and (u_2-u_0) vs (u_1-u_0) Trends

Data from the six (6) CPT soundings were utilized to develop Figure 2. Figure 2a shows the results on the CPT behavior chart proposed by Robertson (2016) which utilizes the normalized corrected tip resistance Q_{tn} and the friction ratio F_r . Data in Figure 2a were color coded as follows: clayey-like materials are represented as blue (i.e., CCS and CC – Contractive) and red (i.e., CD – Dilative); transitional materials are represented as green (i.e., TC – Contractive) and orange (i.e., TD – Dilative); sand-like materials represented as purple (i.e., SC – Contractive) and cyan (i.e., SD – Dilative).

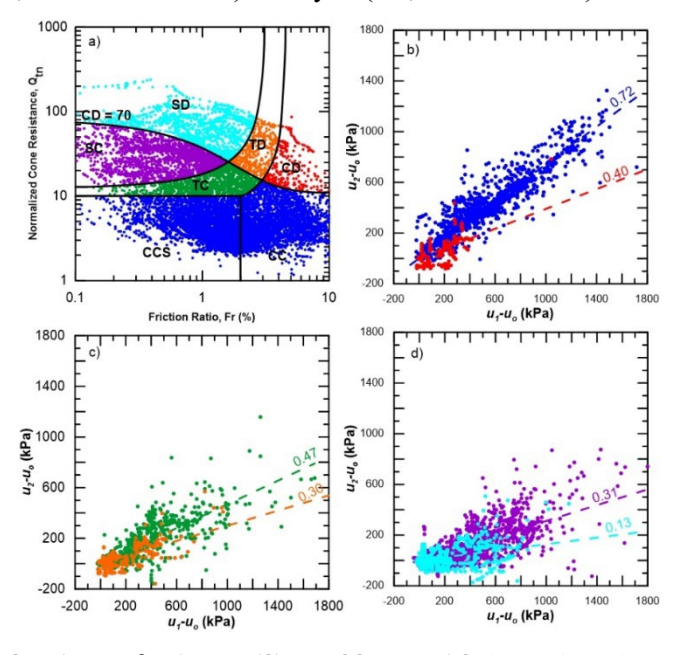


Figure 2: Soil Behaviour of Mine Tailings Along with (u2-u0) vs (u2-u0) for Response

Figure 2b shows the measured pore-water pressure difference (u_2 - u_0) versus (u_1 - u_0) for the clayey-like materials (i.e., CCS–CC and CD) illustrated in blue and red colors, respectively. The CCS–CC data points show some scatter but a clear trend to increase in (u_2 - u_0) with increasing (u_1 - u_0). The average rate of increase for the (u_2 - u_0)/(u_1 - u_0) ratio is 0.72 and the pore-water pressure values are as high as 1,400 kPa. Even though there is a difference in the definition of the ratio, this ratio of 0.72 is close but slightly larger than the ratio (u_2)/(u_1) of 0.70 found by Mayne et al. (1990) for intact clays. The CD data points are much less and show scatter but a trend to increase in (u_2 - u_0) with increasing (u_1 - u_0). The average rate of increase for the (u_2 - u_0)/(u_1 - u_0) ratio is 0.40 which is smaller than the trend for CCS–CC. Furthermore, the highest consistent pore-water pressure values are around 500 kPa. It is anticipated that the measured pore-water pressures in the u_2 and u_1 filter locations for the CD points reflect some negative shear induced pore-water pressure which contributes to these lower pore-water pressure values.

Figure 2c shows the measured pore-water pressure difference (u_2-u_0) versus (u_1-u_0) for the transitional materials (i.e., TC and TD) illustrated in green and orange colors, respectively. The TC data points show significant scatter but trend to increase in (u_2-u_0) with increasing (u_1-u_0) . The average rate of increase for the $(u_2-u_0)/(u_1-u_0)$ ratio is 0.47 and the pore-water pressure values are as high as 1,000 kPa. The TD data points also show scatter and a trend to increase in (u_2-u_0) with increasing (u_1-u_0) . The average rate of increase for the $(u_2-u_0)/(u_1-u_0)$ ratio is 0.30 which is smaller than the trend for TC. Furthermore, the highest consistent pore-water pressure values are around 500 kPa. It is anticipated that the measured pore-water pressures in the u_2 and u_1 filter locations for the TD points reflect some negative shear induced pore-water pressure which contributes to these lower pore-water pressure values. In fact, some of the (u_2-u_0) values are negative in Figure 2c probably reflecting this effect on the measured pore-water pressures.

Figure 2d shows the measured pore-water pressure difference (u_2-u_0) versus (u_1-u_0) for the sandy-like materials (i.e., SC and SD) illustrated in purple and cyan colors, respectively. The SC data points show significant scatter but trend to increase in (u_2-u_0) with increasing (u_1-u_0) . The average rate of increase for the $(u_2-u_0)/(u_1-u_0)$ ratio is 0.31 and the pore-water pressure values are as high as 1,100 kPa. The SD data points are less and show scatter but a trend to increase in (u_2-u_0) with increasing (u_1-u_0) . The average rate of increase for the $(u_2-u_0)/(u_1-u_0)$ ratio is 0.13 which is smaller than the trend for SC. Furthermore, the highest consistent pore-water pressure values are around 800 kPa. It is anticipated that the measured pore-water pressures in the u_2 and u_1 filter locations for the SD points reflect some negative shear induced pore-water pressure which contributes to these lower pore-water pressure values. In fact, some of the (u_2-u_0) values are negative in Figure 2d probably reflecting this effect on the measured pore-water pressures.

Table 1 summarizes the trends for the $(u_2-u_0)/(u_1-u_0)$ ratio found in Figure 2 for the different materials. Table 1 includes the material behavior type, the $(u_2-u_0)/(u_1-u_0)$ ratio, approximately maximum (u_1-u_0) , and color in Figure 2.

Table 1: Summary of the trends for $(u_2-u_0)/(u_1-u_0)$ ratio

MATERIAL	Material Behavior Type	(u ₂ -u ₀)/(u ₁ -u ₀) Average ratio	Approximately Max (u1-u0)	Color
Clay-Like	CCS-CC	0.72	1,400	Blue
	CD	0.40	400	Red
Transitional	TC	0.47	1,000	Green
	TD	0.30	500	Orange
Sand-Like	SC	0.31	1,100	Purple
	SD	0.13	800	Cyan

In general, the trend in Table 1 shows that the $(u_2-u_0)/(u_1-u_0)$ ratio is highest for the clay-like materials and lowest for the sand-like materials, with the transitional materials showing intermediate values. This is attributed to the fact that in clay-like materials penetration takes place under undrained conditions and thus generates higher pore-water pressures during piezocone penetration. In the sand-like materials the penetration tend to be dominated by drained conditions. Within each material-like the contractive materials display a higher $(u_2-u_0)/(u_1-u_0)$ ratio than its dilative counterpart. For example, in the clay-like material (CCS-CC) is greater CD. Similar observation is applicable to transitional (TC>TD) and sand-like (SC>SD) materials. This is attributed to the contribution of the negative pore-water pressures during penetration that are generated in the dilative material.

Pore-water Pressure Dissipation Results

As previously indicated, several PPD tests were conducted during the investigation. Figure 3 shows three typical PPD test results including both (u_2) and (u_I) readings versus time at three different depths. The PPD results at a depth of 11.90 m show almost immediate excess pore-water dissipation when penetration stopped. On the other hand, the PPD results at a depth of 16.15 m show an initial pore-water pressure of approximately 280 kPa (u_I) and 344 kPa (u_2) , respectively. Surprisingly, u_2 started larger than u_I , which can be contributed to the effect of clamping at the beginning of the PPD test. The (u_I) slightly increase followed by a rapid sharp decrease in pore-water pressure to the in-situ value of 103 kPa (u_θ) . The u_2 decreases almost immediately after the penetration stopped. Finally, at a depth of 19.02 m and after the penetration stops, the pore-water pressure first shows a slight increase in magnitude followed by a subsequent decrease of pore-water pressure in time towards the in-situ value.

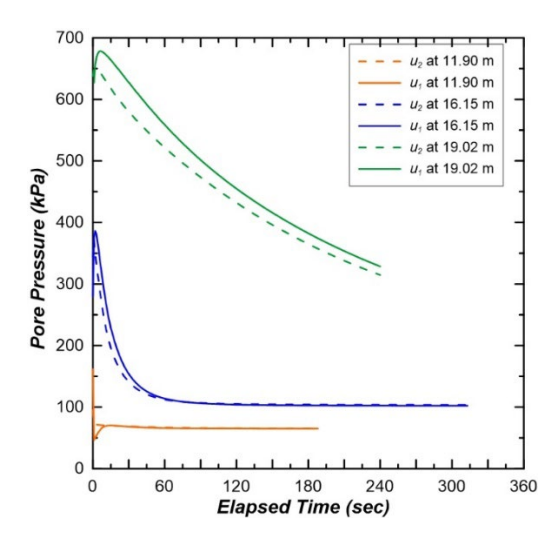


Figure 3: Three Typical PPD Test Results Including Both (u2) and (u1) Readings Versus Time

In all three cases shown in Figure 3, the elapsed time is relatively small and typically less than 300 seconds. The dissipation at 11.90 m is almost immediate while at 16.15 m is a little bit delayed up to about 60 seconds. The dissipation at 19.02 m was stopped before the in-situ value is reached.

Olson (2009) Susceptibility-Compressibility and (u₁-u₀) Trends

Figure 4a shows the results of the measured pore-water pressure at filter location (u_I) during CPT penetration and the in-situ (u_0) pore-water pressure distribution measured with vibratory wire piezometers. It can be seen that except for the upper 2.6 m where predrill occurred and $(u_I) \cong (u_0)$, in general u_I is greater than u_0 . Figure 4b shows the difference (u_I-u_0) versus depth of the same sounding.

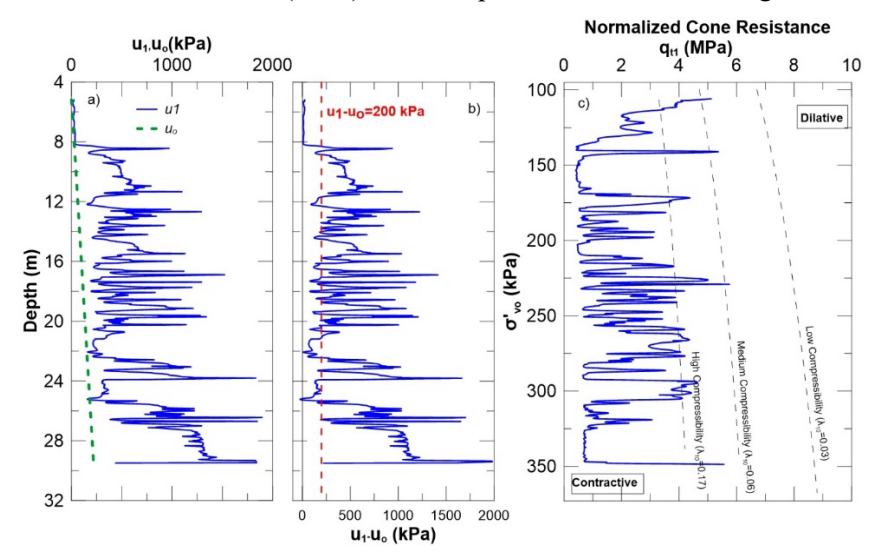


Figure 4: (u_1), (u_0) and (u_1)-(u_0) versus Time and corrected normalized tip resistance q_{t1} versus effective stress σ'_{v_0}

Figure 4c shows the corrected normalized tip resistance q_{tl} versus effective stress σ'_{vo} , of the same CPT sounding as Figures 4a and 4b. Also included in Figure 4c are shown the boundary lines separating dilative from contractive behavior based on compressibility proposed by Olson (2009). The compressibility boundary lines are based on the slope of the critical state line, λ_{10} , and were developed based on estimated compressibility values from case histories. The three compressibilities are associated with a $\lambda_{10} = 0.03$ for low compressibility materials, $\lambda_{10} = 0.06$ for medium compressibility materials, and $\lambda_{10} = 0.17$ for high compressibility materials.

The mine tailings associated with the facility reflected in the CPT in Figure 4 are classified as high compressibility with λ_{10} ranging within 0.10-0.20. Most of the sounding shown the corrected normalized tip resistance q_{tl} is on the contractive side of High Compressibility Boundary line. It is interesting to note that there are some corrected normalized tip resistance q_{tl} values that are on the dilative side of the boundary line. Furthermore, the zones where q_{tl} falls on the dilative side correspond to depths (i.e., effective stresses) in Figure 4b in which the difference (u_1 - u_0) is less than approximately 200 kPa.

On a preliminary basis, the line for the difference (u_1-u_0) of 200 kPa appears to be related to the boundary line separating dilative from contractive behavior of high compressible mine tailings. Further assessment is warranted to provide firm evidence in this observation.

Summary and Conclusions

The results of a comprehensive field investigation program conducted across three (3) different tailings storage facilities (TSFs) using CPT with dual pore-water pressures filter element locations (u_1 and u_2) and presented and discussed. Typical CPT results with dual filter elements are presented and relevant features are highlighted in relation to tailings characterization, state, aging, and stress history as well as other behavior factors. The following presents summary and the conclusions of the work:

- 1) Figure 2a summarizes the results of the 6 CPT with dual filter elements at the three TSF using Robertson (2016) behavior classification chart.
- 2) Figure 2b through 2d summarizes the general trends for $(u_2-u_0)/(u_1-u_0)$ ratio and Table 1 summarizes the numerical values. In general, $(u_2-u_0)/(u_1-u_0)$ ratio is highest for the clay-like materials and lowest for the sand-like materials, with the transitional materials showing intermediate values.

- 3) Within each material-like the contractive materials display a higher $(u_2-u_0)/(u_1-u_0)$ ratio than its dilative counterpart. This is attributed to the contribution of the negative pore-water pressures during penetration that are generated in the dilative material.
- 4) The overall dissipation behavior in the CPT with dual filter element is similar to the observed in regular CPT piezocone.
- 5) Figure 4c summarizes the results from one CPT in terms of the corrected normalized tip resistance q_{tl} versus effective stress s'_{vo} , including the boundary lines separating dilative from contractive behavior based on compressibility proposed by Olson (2009).
- 6) Figure 4b suggests that the difference $(u_I u_0)$ of 200 kPa appears to be related to the boundary line separating dilative from contractive behavior of high compressible mine tailings. Additional assessment is needed in this aspect.
- 7) Pending additional analysis, other pore-water differences (u_1-u_0) could be related to state parameter.

The authors continue performing additional assessments of the data with the purpose of establishing other possible correlations. Those results will be presented in future publications.

References

- Baligh, M.M. 1986. Undrained deep penetration, II: pore pressures. Géotechnique, 36(4): 487–501.
- Burns, S.E. and Mayne, P.W. 1998. Monotonic and dilatory pore pressure decay during piezocone tests. Canadian Geotechnical Journal 35 (6), 1063-1073.
- Campanella, R.G., Robertson, P.K., and Gillespie, D. 1986. Factors affecting the pore water pressure and its measurement around a penetrating cone. *In* Proceedings, 39th Canadian Geotechnical Conference, Ottawa, pp. 291–299.
- Campanella, R.G. and Robertson, P.K. 1988. Current status of the piezocone test. Penetration Testing 1988 (1), Balkema, 93-116.
- Contreras, I.A. and Grosser, A.T. 2009. Evaluation of CPT response under fast penetration rate in silty soils. In Proceedings of the 57th Annual Geotechnical Engineering Conference. Minneapolis, Minnesota, February 2009.

- Contreras, I.A. and Harvey, J.W. 2021. The role of the vane shear test in mine tailings. *Proceedings of Tailings and Mine Waste 2022*.
- Jamiolkowski, M., Ladd, C.C., Germaine, J.T., and Lancellotta, R., 1985. New developments in field and laboratory testing of soils. In Proceedings of the 11th International Conference on Soil Mechanics and Foundation Engineering. San Francisco, California, August 1985, Vol.1 pp. 57-153.
- Lunne, T., Powell, J., & Robertson, P. E. T. E. R. (1996). Use of piezocone tests in non-textbook materials. In advances in site investigation practice. proceedings of the international conference held in London on 30-31 march 1995.
- Mayne, P. W., Kulhawy, F. H., & Kay, J. N. 1990. Observations on the development of pore-water stresses during piezocone penetration in clays. *Canadian Geotechnical Journal*, *27*(4), 418-428.
- Olson, S. M. 2009. Strength ratio approach for liquefaction analysis in tailings dams. In Proceedings of the 57th Annual Geotechnical Engineering Conference. Minneapolis, Minnesota, February 2009.
- Robertson, P.K. 2016. Cone penetration test (CPT)-based soil behaviour type (SBT) classification system an update. Canadian Geotechnical Journal, 53(12): 1910–1927. doi:10.1139/cgj-2016-0044
- Terzaghi, K., Peck, R. B., & Mesri, G. 1996. Soil mechanics in engineering practice. John wiley & sons.
- Wroth, C.P. 1984. The interpretation of in-situ soil tests: 24th Rankine Lecture. Géotechnique, 34(4): 449–489.